Electronic Supplementary Information (ESI)

Reducing Lithium Deposition Overpotential with Silver Nanocrystals Anchored on Graphene Aerogel

Xianshu Wang,[a] Zhenghui Pan,[b] Yang Wu,[c] Guoguang Xu,[b] Xiongwen Zheng,[a] Yongcai, Qiu,[d] Meinan Liu,[b] Yuegang Zhang,[bc*] Weishan Li[ae*]

[a] School of Chemistry and Environment, South China Normal University, Guangzhou 510006, China

[b] *i*-lab, Suzhou Institute of Nano-Tech and Nano-Bionics, Chinese Academy of Sciences Suzhou, Jiangsu 215123 , China

[c] Department of Physics, Tsinghua University, Beijing 100084, China

[d] School of Environment and Energy, South China University of Technology, Guangzhou 510006, China

[e] Engineering Research Center of MTEES (Ministry of Education), Research Center of BMET (Guangdong Province), and Key Laboratory of ETESPG (GHEI), South China Normal University, Guangzhou 510006, China

* Corresponding author: liwsh@scnu.edu.cn; yuegang.Zhang@tsinghua.edu.cn;

1. Experimental Section

1.1 Synthesis of graphene oxide (GO)

GO was synthesized according to Xu et al.[1] Firstly, natural graphite powder (10 g) was put into a flask with a solution containing concentrated H_2SO_4 (30 mL), $K_2S_2O_8$ (10 g) and P_2O_5 (10 g), and the mixture was then kept at 80 °C for 6 h. After cooling to room temperature, deionized (DI) water was added to wash the resultant, followed by filtration and vacuum drying. Secondly, the resulting graphite oxide was oxidized further by a modified Hummers' method. Graphite oxide (2.0 g) was put into a flask with concentrated H_2SO_4 (48 mL) in an ice bath (0 °C), and then $KMnO_4$ (6 g) was gradually injected under vigorous stirring to react for 1 h. The resultant mixture was stirred for oxidation at 35 °C for 2 h, and then diluted with DI water (96 mL) added in a dropwise manner. Subsequently, the mixture was further oxidized at 98 °C for 0.5 h with stirring. After cooling to room temperature, 25 mL 30% H_2O_2 was added to eliminate the residual $KMnO_4$ after dilution with additional 100 mL DI water. Afterwards, the product was washed with 5 wt. % HCl (187.5 mL) to remove metal ions, followed by centrifuging and washing with DI water until neutral. Finally, dialysis was carried out to further remove the impurity.

1.2 Fabrication of aerogels with/without silver nanocrystals

$AgNO_3$ (Sinopharm, 0.1 mmol) and Vitamin C (Sigma-Aldrich, 0.05 mmol) were dissolved in GO aqueous solution (2 mg mL^{-1}, 10 mL) in turns, followed with hydrothermal in a sealed cylindrical vessel at 180 °C for 2 h. After freeze-drying, the resultant graphene hydrogel (GH) became into graphene aerogel (GA) loaded with silver nanocrystals (AgNCs) (denoted as AgNCs@GA). The pure GA without AgNCs (denoted as GA) was obtained by identical process mentioned above except for no

addition of $AgNO_3$, used as a reference.

1.3 Ag or Cu foil treatment

Cu foil was pre-treated in a diluted hydrochloric acid under ultrasonication to remove surface oxide, and then washed to neutral and dried by vacuum oven. When tested as the base control, it was firstly cycled in the voltage of 0 ~ 1 V for 10 times to remove the surface contaminant and stabilize the interface at 0.1 C (1 C = 1000 mA g^{-1}) before electrochemical measurements (Figure S13, ESI†). Ag foil as substrate for verifying the overpotential was acquired by thermal evaporation in a vacuum chamber, and its thickness was controlled at 300 nm.

1.4 Physical characterizations

Scanning electron microscopy (SEM) was performed on a cold field-emission scanning electron microscopy (Hitachi S4800, Japan) and an environmental scanning electron microscopy (FEI Quanta 250, America). X-ray diffraction (XRD) was collected with a powder diffractometer (Bruker D8 Advanced, Germany). Transmission electron microscopy (TEM) was performed on a field-emission transmission electron microscope (FEI Tecnai G2 F20 S-Twin, America). X-ray photoelectron spectroscopy (XPS) was performed using a spectrometer with Al kα X-ray source (Thermo Scientific Escalab 250XI, America). Brunauer-Emmett-Teller (BET) nitrogen adsorption-desorption isotherm measurement was carried out by a specific surface area analyzer (Gold APP V-sorb 2800, China).

1.5 Electrochemical measurements

Electrochemical measurements were carried out using a Land automatic battery tester (Land CT2001, China) and a multi-channel electrochemical workstation (Bio-logic VMP3, French) in CR2025 coin-type cells. To prepare the electrodes, aerogels powder and polyvinylidene fluoride binder

(PVDF) (aerogels powder:PVDF = 85:15, by weight) were mixed with N-methylpyrrolidone (NMP) to form a slurry by stirring overnight. The slurry was then coated on a Cu foil and dried in a vacuum oven at 60 °C overnight. The electrode was punched into disks (diameter = 15 mm, an areal mass loading of 0.5732 mg cm^{-2} with about 1.8 wt. % Ag). Ag is expensive but such a low Ag content does not add high cost to the electrode. Li foil (Shenzhen Kejingstar Technology Ltd., thickness = 450 μm) was employed as the counter electrode. 1.0 mol L^{-1} LiTFSI in DOL/DME (1:1, by volume) with 1% $LiNO_3$ (ether-based) or 1.0 mol L^{-1} $LiPF_6$ in EC/EMC/DEC (3:5:2, by weight, carbonate-based) was used as electrolyte. All the tests were performed in ether-based electrolyte unless otherwise indicated. Similarly, $LiFePO_4$ cathodes were prepared by mixing $LiFePO_4$, acetylene black, and PVDF in a ratio of 8: 1: 1 into a slurry in NMP, followed by coating on Al foil and vacuum drying. The as-obtained $LiFePO_4$ cathode was also punched into disks (diameter = 15 mm, areal mass loading of 2.18 or 6.0 mg cm^{-2}). All coin cells were tested in galvanostatic mode. For columbic efficiency (CE) test, the depositing process was fixed by controlling the time for quantitative lithium, but the stripping process was only controlled by a cut-off voltage of 1.2 V (*vs.* Li^+/Li) without time limit. For $LiFePO_4$-based full battery (1C = 170 mA g^{-1}), galvanostatic charge/discharge was performed within a voltage range of 2.2 V to 4.1 V. Electrochemical impedance spectroscopy (EIS) was performed after discharge in a frequency range from 200 kHz to 10 mHz with a voltage amplitude of 10 mV.

1.6 Theoretical calculations

The calculations were based on density functional theory (DFT) method as implemented in the Vienna ab initio simulation package (VASP).[2, 3] The exchange-correlation function was treated to describe the interactions within generalized gradient approximation (GGA) in the Perdew-Burke-Ernzerhof formalism (PBE).[4] Spin-polarized magnetic calculations using 'accurate' precision and a

user-defined plane wave cut-off energy of 500.000 eV were employed to ensure accurate energies with less than 1 m eV per atom.[5] The electronic iterations convergence is 1.00×10^{-5} eV using the Normal (blocked Davidson) algorithm and reciprocal space projection operators. Binding energy (E_b) was calculated by subtracting the energies of gas phase species and the clean surface from the total energy of the adsorbed system; $E_b = E(Li/slab) - [E(Li) + E(slab)]$, and a more negative E_b indicates a more stable combination or higher Li affinity.

2. Supplementary Figures

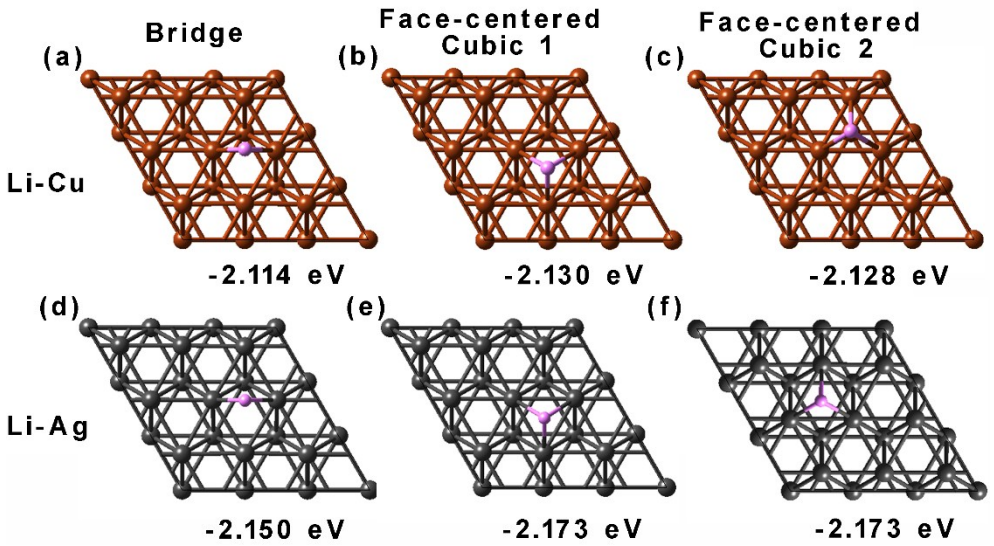

Figure S1. The calculated binding energy of a Li atom with (a-c) Cu or (d-f) Ag in the different combination mode: (a, d) bridge, (b, e) face-centered cubic 1, and (c, f) face-centered cubic 2. In either mode, the binding energy of Li-Ag is higher than that of Li-Cu, indicative of Ag slab has a high Li affinity.

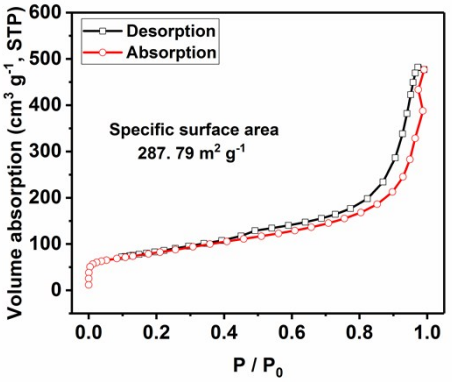

Figure S2. Nitrogen adsorption-desorption isotherm collected at liquid nitrogen temperature (77 K) for AgNCs@GA. Its high specific surface area (287.79 m^2 g^{-1}) is derived from three-dimensional porous structure.

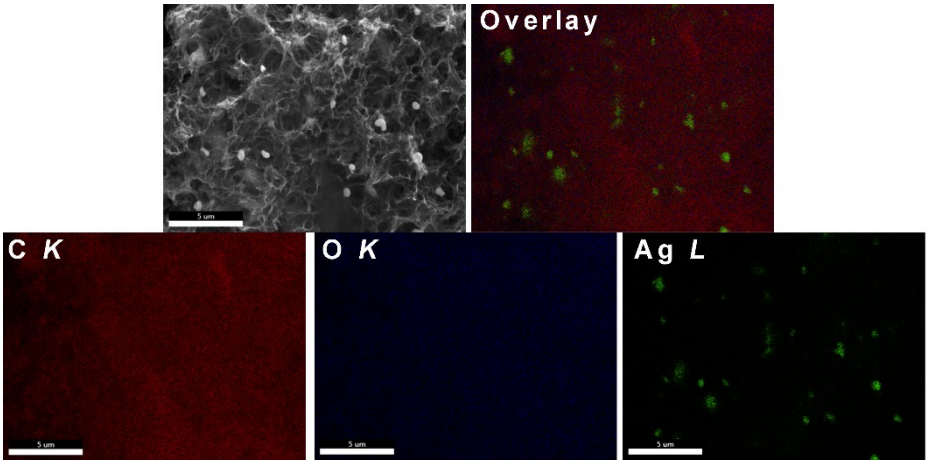

Figure S3. SEM image of AgNCs@GA and the corresponding energy-dispersive X-ray (EDX) elemental mappings of C, O and Ag.

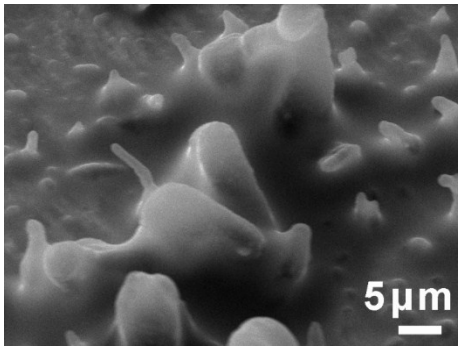

Figure S4. SEM image of bare Cu electrode after Li deposition with a capacity of 2.0 mA h cm^{-2} from sectional view, which further reveals dendrite formation and growth.

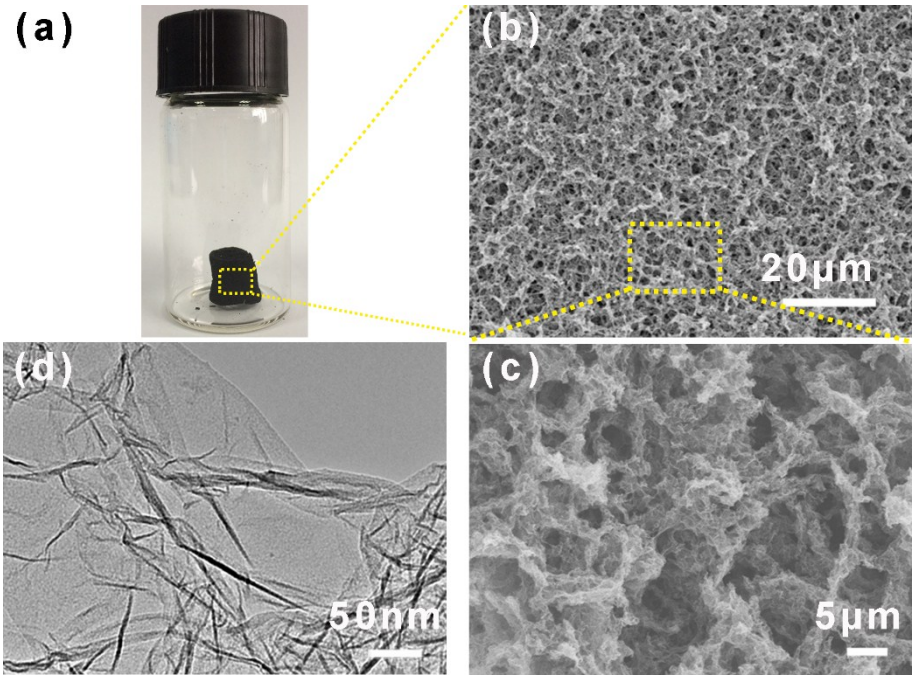

Figure S5. (a) Digital photo, (b, c) SEM and (d) TEM images of as-synthesized GA.

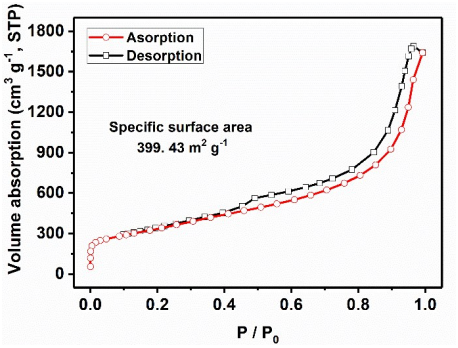

Figure S6. Nitrogen adsorption-desorption isotherm of GA, collected at liquid nitrogen temperature (77 K).

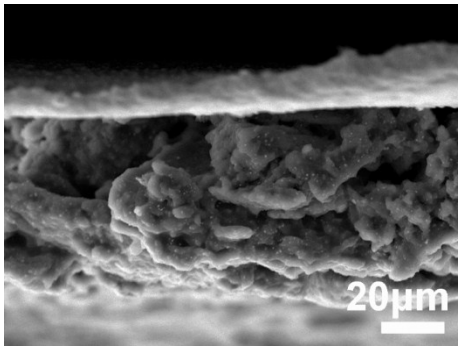

Figure S7. SEM image of AgNCs@GA-modified electrode with Li deposition under sectional view, which further demonstrates a dendrite-free morphology.

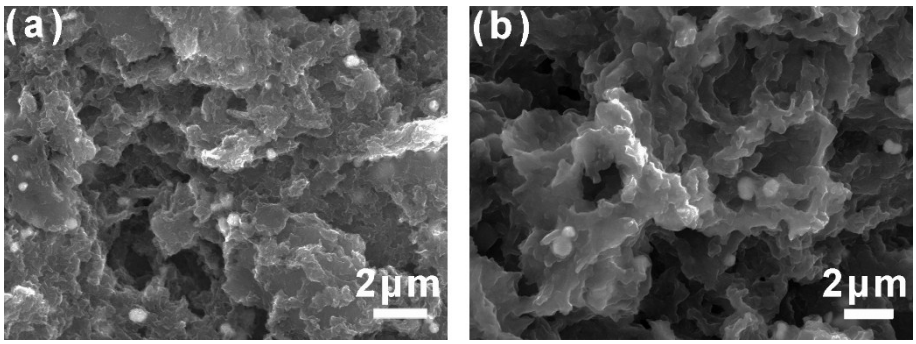

Figure S8. SEM images of 3D AgNCs@GA-modified electrode after (a) the 1st and (b) the 30th Li stripping.

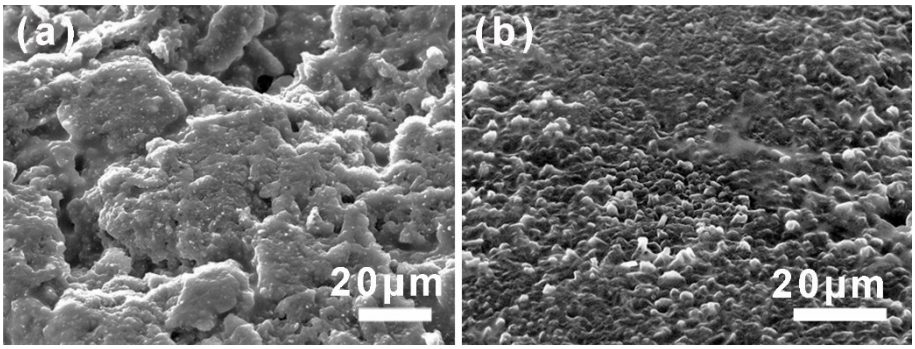

Figure S9. Side-view SEM images of AgNCs@GA-modified electrode with Li capacities of (a) 2.0 and (b) 5.0 mA h cm^{-2}.

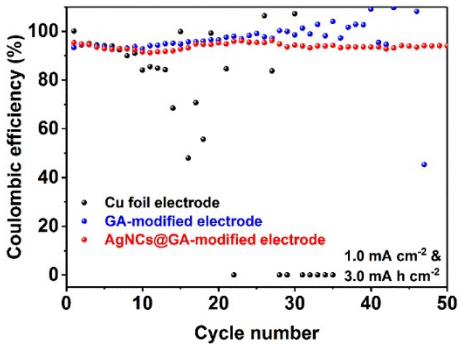

Figure S10. Coulombic efficiencies of bare Cu, GA-modified and AgNCs@GA-modified electrodes with areal capacity of 3.0 mA h cm^{-2} at a current density of 1.0 mA cm^{-2}.

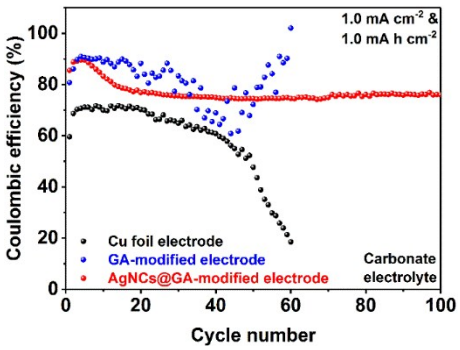

Figure S11. Coulombic efficiencies of Cu foil, GA-modified and AgNCs@GA-modified electrodes in carbonate-based electrolyte (1.0 mol L^{-1} $LiPF_6$ in EC/EMC/DEC (3:5:2, by weight)) with 1.0 mA h cm^{-2} Li capacity at 1.0 mA cm^{-2}.

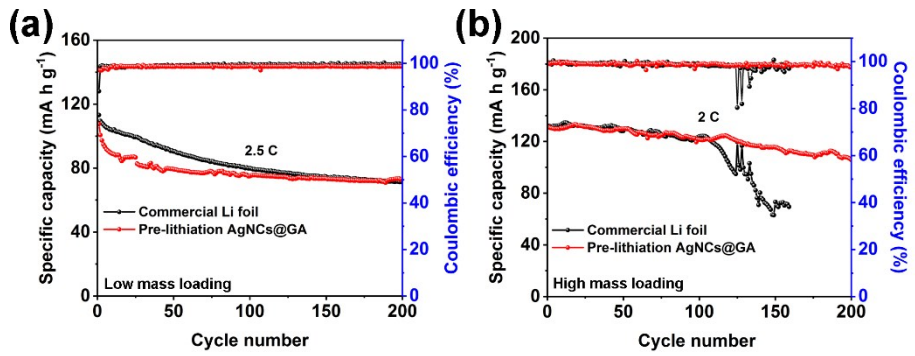

Figure S12. Cyclic stability of pre-lithiated AgNCs@GA-modified anode paired with $LiFePO_4$ cathode with mass loadings of (a) 2.18 mg cm^{-2} at 2.5 C and (b) 6.0 mg cm^{-2} at 2 C, with a comparison of commercial Li foil.

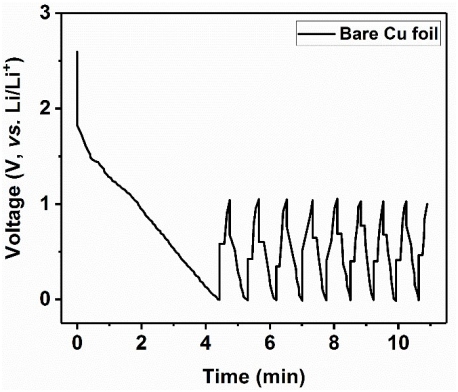

Figure S13. The pre-cycled voltage profiles of bare Cu electrode before CE test in a voltage of 0 ~ 1 V (*vs.* Li/Li^+) at 0.1 C (1 C = 1000 mA g^{-1}) for 10 times.

References

1 Z. Xu, and C. Gao, *ACS Nano,* 2011, **5**, 2908.

2 G. Kresse, and J. Furthmüller, *Comput. Mater. Sci.,* 1996, **6**, 15;

3 G. Kresse, and J. Furthmüller, *Phys. Rev. B*, 1996, **54**, 11169.

4 J. P. Perdew, K. Burke, and M. Ernzerhof, *Phys. Rev. Lett.,* 1996, **77**, 3865.

5 M. Methfessel, and A. Paxton, *Phys. Rev. B,* 1989, **40**, 3616.